The optical design of the G-CLEF Spectrograph: the first light instrument for the GMT

Ben-Ami, Sagi, Crane, Jeffrey, Evans, Ian, McMuldroch, Stuart, Mueller, Mark, et al.

Sagi Ben-Ami, Jeffrey D. Crane, Ian Evans, Stuart McMuldroch, Mark Mueller, William Podgorski, Andrew Szentgyorgyi, "The optical design of the G-CLEF Spectrograph: the first light instrument for the GMT," Proc. SPIE 10702, Ground-based and Airborne Instrumentation for Astronomy VII, 107029K (12 July 2018); doi: 10.1117/12.2313381

SPIE.

Event: SPIE Astronomical Telescopes + Instrumentation, 2018, Austin, Texas, United States

The optical design of the G-CLEF Spectrograph: the first light instrument for the GMT

Sagi Ben-Ami[a], Jeffrey D. Crane[b], Ian Evans[a], Stuart McMcmuldroch[a], Mark Mueller[a], William Podgorski[a], Andrew Szentgyorgyi[a]

[a]Harvard-Smithsonian Center for Astrophysics, 60 Garden St., Cambridge, MA 02140; [b]UCO/Lick Observatory, University of California, Santa Cruz, CA 95064

[b]The Observatories of the Carnegie Institution for Science, 813 Santa Barbara Street, Pasadena, CA 91101

Abstract

The GMT-Consortium Large Earth Finder (G-CLEF), one of the first light instruments for the Giant Magellan Telescope (GMT), is a fiber-fed, high-resolution echelle spectrograph. G-CLEF is expected to proceed towards fabrication in the coming months. In this paper, we present the current, pre-construction G-CLEF optical design, with an emphasis on the innovative features derived for the spectrograph fiber-feed, the implementation of a volume-phase holographic (VPH)-based cross disperser with enhanced blue throughput and our novel solutions for a multi-colored exposure meter and a flat-fielding system.

Keywords: GMT, ELT, Echelle, Spectrographs, PRV, Exoplanets.

INTRODUCTION

G-CLEF (GMT-Consortium Large Earth Finder) [1] is among the first light instruments for the Giant Magellan Telescope (GMT) [2]. It is being built by an international consortium of GMT members. G-CLEF, an ultra-stable and versatile high resolution spectrograph, operates in the visible band ($\lambda \sim 350 - 950\text{nm}$) and offers several observing modes, ranging from a high throughput, resolution (R) = 20,000 mode to a pupil-sliced, R=108,000 mode. In addition, G-CLEF can be used as a multi-object spectrograph when fed through the GMT Many Instrument Fiber System (MANIFEST) [3].

Key G-CLEF science cases include precision radial velocity (PRV) measurements for exoplanet host stars, the characterization of exoplanet atmospheres, the study of low metallicity stars in the galaxy halo, internal dynamics of dwarf galaxies in the local group, and the study of high redshift quasars through Lyα absorption systems.

G-CLEF is mounted on the gravity-invariant azimuth disk of the telescope, inside a thermally controlled vacuum vessel [4]. Light from the GMT is fed into the instrument through a system of optical fibers, the terminus of which ends inside the spectrograph forming the instrument pseudo-slit. The input beams are collimated by an off-axis-parabolic (OAP) mirror, and are dispersed by a mosaic of echelle gratings. The dispersed beams are refocused by the OAP mirror in a second pass and are reflected by a Mangin Mirror towards a second collimator, where they are re-collimated by a second conic mirror. A dichroic splits the re-collimated beams into a blue channel ($350 - 540\text{nm}$), and a red channel ($540 - 950\text{nm}$). Two echellograms are then reimaged onto two large format CCDs by 8- and 7-elements cameras for the blue and red channels, respectively [5].

The technical requirements for building a versatile, broad band high resolution spectrograph with extreme PRV capabilities are extremely demanding [6]. They are exceeded by those in the case of G-CLEF, one of the first instruments designed for the next generation of Extreme Large Telescopes (ELTs). In many cases, this has led us to develop unique solutions to optical and mechanical challenges raised during the design process. In this paper we present the pre-construction optical design of G-CLEF, with an emphasis on some of these unique solutions, such as the multi-mode spectrograph fiber-feed, the implementation of a VPH cross disperser coupled to a pre-dispersing prism to increase efficiency, our novel solutions for a multi-colored exposure meter, and the flat fielding system. The paper is split into two sections. The first section is dedicated to the fiber system which channels light from the telescope focal plane down to the spectrograph quasi-slit inside the vacuum enclosure. The second section is dedicated to the spectrograph optical design. This paper is a part of a series of manuscripts dedicated to G-CLEF published in this proceedings [7-11].

Ground-based and Airborne Instrumentation for Astronomy VII, edited by Christopher J. Evans, Luc Simard, Hideki Takami, Proc. of SPIE Vol. 10702, 107029K · © 2018 SPIE · CCC code: 0277-786X/18/$18 · doi: 10.1117/12.2313381

2. FIBER SYSTEM

The G-CLEF fiber system is divided into four subsystems shown schematically in Figure 1. The Fiber Run subassembly and Fiber Feed subassembly include the science and sky fibers. The Fiber Run subassembly includes the optical units feeding the science and sky fibers, while the Fiber Feed subassembly generates the spectrograph quasi-slit. The optical fibers of the two systems are fused together in front of the vacuum vessel. An additional subassembly is the Calibration Fiber Run, which includes the calibration light injectors units, the Flat field unit and the Exposure Meter Unit. Finally, the MANIFEST Interface Subassembly connects G-CLEF to the MANIFEST instrument and generates the spectrograph quasi-slit for the multi object spectroscopy (MOS) mode.

The science and sky fibers are grouped together according to the four observing modes behind four Fiber Mirrors onto which the telescope image is relayed, see Figure 2. Three holes, one in the mirror center and one to each side, allow transmission of the object and sky patches downstream, while reflecting the rest of the field of view to the flexure control camera (FCC) – which functions as the instrument guiding camera [11]. The selection between modes is done by linear translation of the platform so that the desired observing mode is in-line with the relayed telescope image. The core diameters of the fibers of each mode differs, and determines the resolution for a given mode, see Table 1.

Table 1: G-CLEF Resolution Modes: Precision Radial Velocity (PRV), Non Scrambled Precision Radial Velocity (NS-PRV), Medium Resolution (MR), and High Throughput (HT).

Mode	Resolution	Fiber	#Science Fibers	#Calib/Sky Fibers	Comments
PRV	108,000	Hexagonal 100μm Core	7	2	Precision Radial Velocity
NS-PRV	108,000	Circular 100μm Core	7	2	Non-Scramble PRV
MR	35,000	Circular 300μm Core	1	2 (+1 GMTNIRS)	Medium Resolution
HT	19,000	Circular 450μm Core	1	2 (+1 GMTNIRS)	High Throughput

2.1 Feeding the G-CLEF Sky and Science Fibers.

The GMT relayed image is at an F/8. This is not ideal for feeding optical fibers, as losses induced by focal ratio degradation (FRD) are expected to be substantial at such high F-numbers [12,13]. Therefore, all optical fibers dedicated to sky calibration, as well as MR and HT mode science fibers go through a focal reducer. In order to eliminate an air-to-glass interface, we choose to bond the fibers directly to the last optical element in the focal reducer. Hence, the focal reducers are bi-telecentric relay systems with m=3/8 magnification and zero back focal distance, see Figure 3.

For seeing limited spectrographs, given a constant slit width, the characteristic disperser dimension is proportional to the telescope diameter. For the next generation ELTs this impose a substantial problem, as the size of the instruments becomes unfeasible. To alleviate the problem while obtaining the required resolution of $\mathcal{R}\sim100{,}000$, relevant to G-CLEF key science objectives, the PRV and NS-PRV modes are pupil sliced. This reduces the required size if the echelle grating, which in turn is proportional to the effective size of the primary mirror [14]. An optical layout of the pupil slicer is shown in Figure 4. The F/8 beam from the telescope expands and is collimated by a doublet lens. The GMT pupil is realized one focal distance from the collimating lens, where it is sliced into seven sub-apertures by seven doublets. The seven doublets have a flat back surface, and are cemented to a common fused silica block. The collimated beam of each aperture is focused on the polished back of the common block at F/3, and is captured on a cemented fiber face.

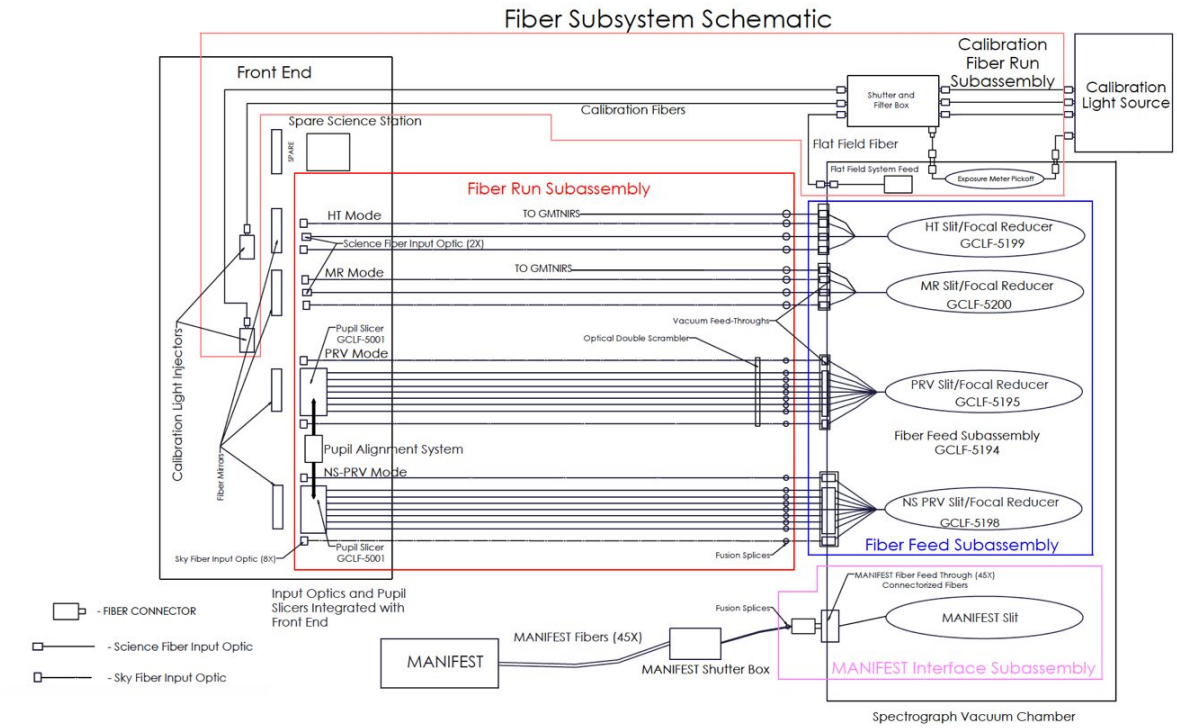

Figure 1: Fiber System Layout

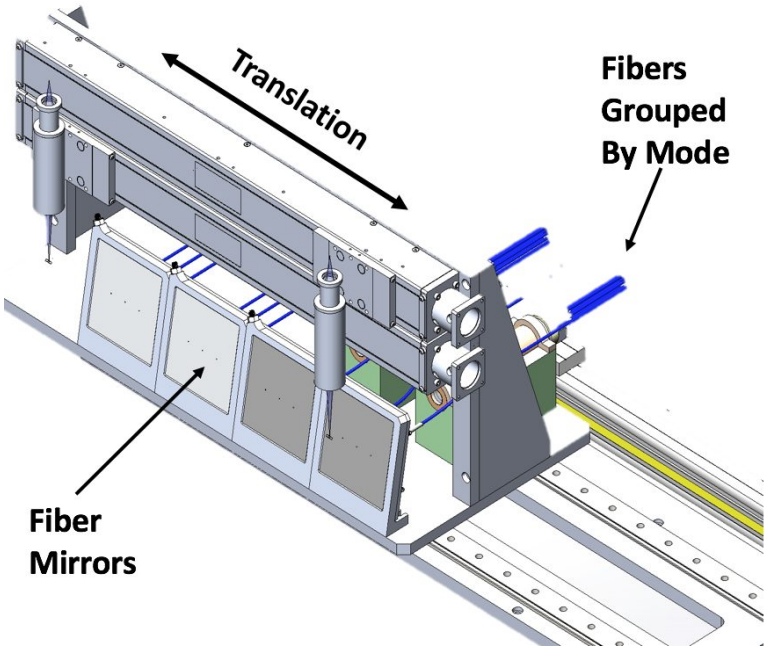

Figure 2: Fiber Mirrors and Observing Mode Selection Platform.

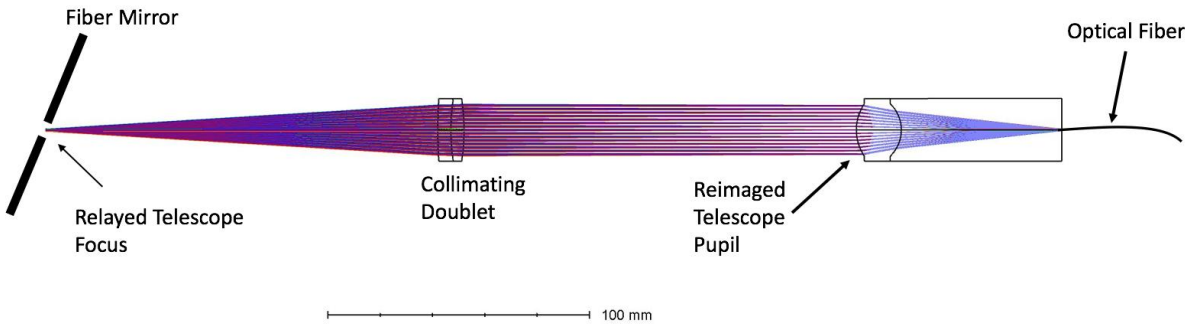

Figure 3: Sky / HT / MR modes Focal Reducers.

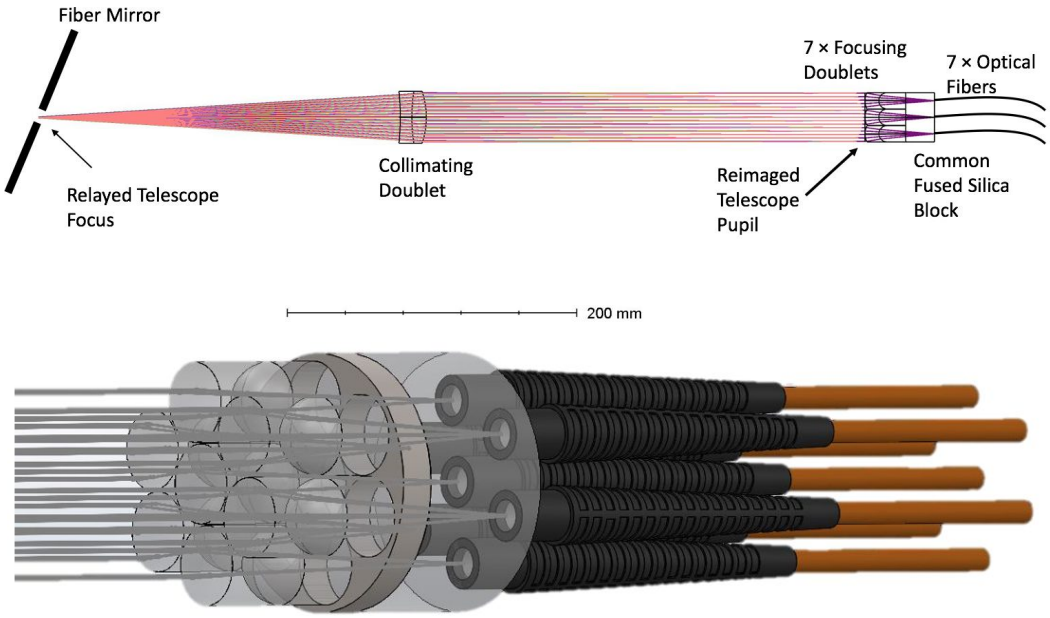

Figure 4: G-CLEF Pupil Slicer Units for the PRV and NS-PRV modes. Top: Optical Layout; Bottom: The Slicing Unit.

The pupil slicer design offers the following benefits:

1. Takes advantage of the GMT discontinuous pupil.
2. A minimal number of air-to-glass interfaces.
3. Each fiber can be accurately and individually positioned to allow capture of the focused beam from each of the sub-apertures.
4. The Focusing Optics Assembly with 7 jacketed cables (approximately 15 meters long) can be spared as a unit.

In addition, a Pupil Alignment (PA) Module can be positioned downstream of the collimating doublet. The PA module picks the beam from either the PRV or NS-PRV modules using a pellicle and a mirror arranged as a periscope. The pellicle allows part of the beam to be fed into the spectrograph during alignment, which allows us to measure efficiency as a function of the focusing module rotation around the pupil slicer optical axis. The optical layout of the PA module is shown in Figure 5 left panel. Once the beam is folded into the PA module, it is partitioned by a beam splitter which

directs part of the beam onto a flat mirror, while the remaining part is directed towards a spherical mirror. As the two beams are combined in a second pass through the beam splitter, the telescope pupil and the telescope focus are reimaged on a common plane (i.e., the beam reflected by the flat mirror realizes the telescope pupil while the beam reflected by the spherical mirror reimages the telescope focus), see Figure 5 right panel. The common focus plane is then reimaged by an off-the-shelf machine vision lens onto a CMOS detector. By imaging both the telescope pupil and focus to a common plane, the PA module allows us to detect tilt and decenter between the telescope and the pupil slicers optical axes, as well as telescope defocus on the Fiber Mirrors.

2.2 Injection Unit

The science and sky fibers for each mode are ganged together and input into a single Injection Optics Assembly. The function of the injection module is twofold:

1. Format the individual fibers into a pseudo-slit.
2. Convert the F/3 fiber output into an F/8 output beam suitable for injection into the spectrograph.

The pseudo-slit configuration for the four G-CLEF modes is illustrated in Figure 6. The PRV mode pseudo-slit is centered on the optical axis. The NS-PRV mode slit is to the left of the PRV mode. The MR mode and HT mode pseudo-slits are arranged to the right of the PRV mode, within the 30mm diameter which indicates acceptable fiber image quality. The MANIFEST fibers are shown to the left of the G-CLEF pseudo-slit.

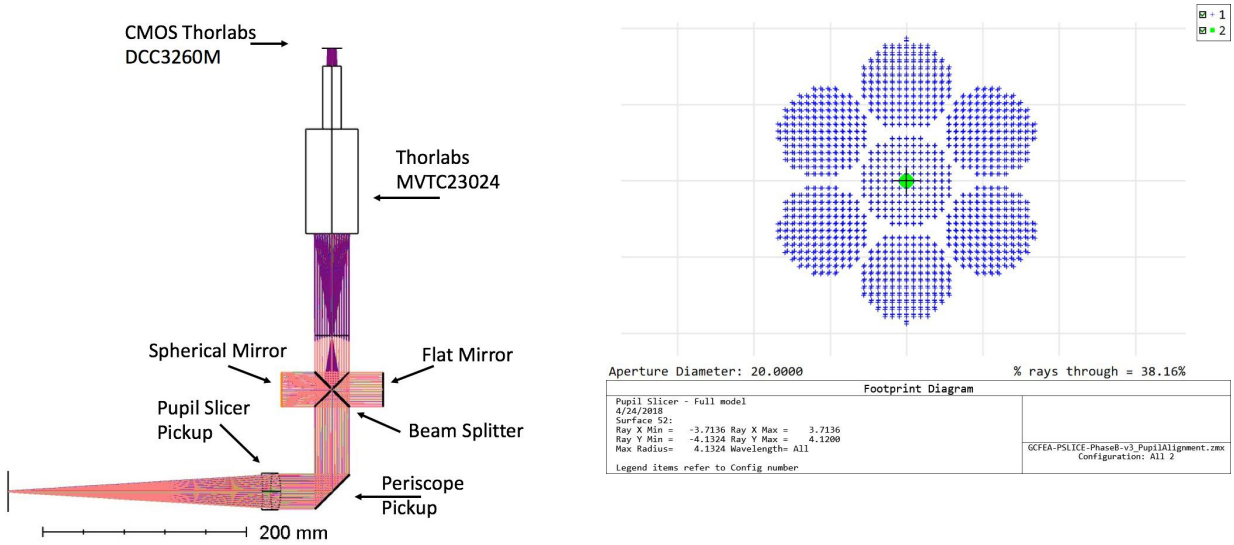

Figure 5: Pupil Alignment Module. Left: Optical Layout; Right: PA Module Image Plane. The blue dots represent the telescope pupil, while the green dot represent the telescope focus.

The beam emitted from each fiber has an F/3 speed (FRD will increase the speed at which the output beam diverges, but we intend to mask rays outside of the F/3 cone). This beam divergence must be reduced to that of an F/8 beam. This is achieved by focal ratio conversion lens assemblies which reimage the fibers faces to a common quasi-slit plane located at the focal plane of the spectrograph collimator, see section 3. In order to eliminate an air-to-glass interface, the fibers are cemented to the front surface of the optical system. The injection optics is therefore a bi-telecentric $m = 8/3$ with zero front focal distance. A ZEMAX model of the focal ratio reducer output lens assembly is shown in Figure 7.

2.3 The Flat Field Injector

In many modern PRV echelle spectrographs, calibration of pixel-to-pixel efficiency variations is achieved by using a large core diameter fiber, which is imaged into a trace wider (in the cross dispersion direction) than the one created by the science fiber [6,15]. This allows high and uniform photon flux across pixels that are not well illuminated by the science fibers (i.e., inter- and intra-order spacing), and a calibration of the PSF wings at the cross-dispersion direction. Care must be taken when choosing the fiber to not overlap traces between orders. Therefore, the correct fiber will be on

one hand large enough to sample pixels at the edge of the science trace with a high photon flux, yet not larger than the order separation in the cross-dispersion direction.
While this method is relatively simple to implement in many echelle spectrographs, in the case of G-CLEF, the slit length (for the PRV mode) is $\sim 1.3\text{mm}$ at the $F/3$ plane ($\sim 3.44\text{mm}$ at the $F/8$ plane), and therefore a fiber large enough to accommodate the entire slit is not feasible. We therefore adopt a solution that will create a large enough uniform slit at the $F/8$ quasi-slit plane, with the correct angular divergence of the $F/8$ beam going into the spectrograph to allow calibration of the pixel-to-pixel variation.

Our solution is based on utilizing an industrial diffuser. When such a diffuser is fed with a parallel beam, each point on the diffuser will generate a telecentric source with a divergence according to the diffuser properties. However, due to imperfections in the diffuser, the beam divergence from each point will not be uniform[1]. Placing the diffuser at the focal plane of a lens system, so that a pupil is generated at the back focal distance of the lens system, we can control the divergence angle from each point, and generate a uniform slit image, see Figure 8. The angular divergence from each point in the pupil, as well as the pupil size, will be determined by the size of the beam collimated onto the diffuser, and the lens system properties. Table 2 details G-CLEF flat field projector optical prescription. At the configuration depicted in the Table, a $0.25\times3.6\text{mm}$ uniform slit image is created at the spectrograph quasi-slit plane (i.e., the image plane of the injection optics), with a uniform angular distribution between $-3.7° < \theta < 3.7°$, similar to an $F/7.7$ beam. The mechanical design of the projector will follow closely that of the injection optics units described in section 2.2.

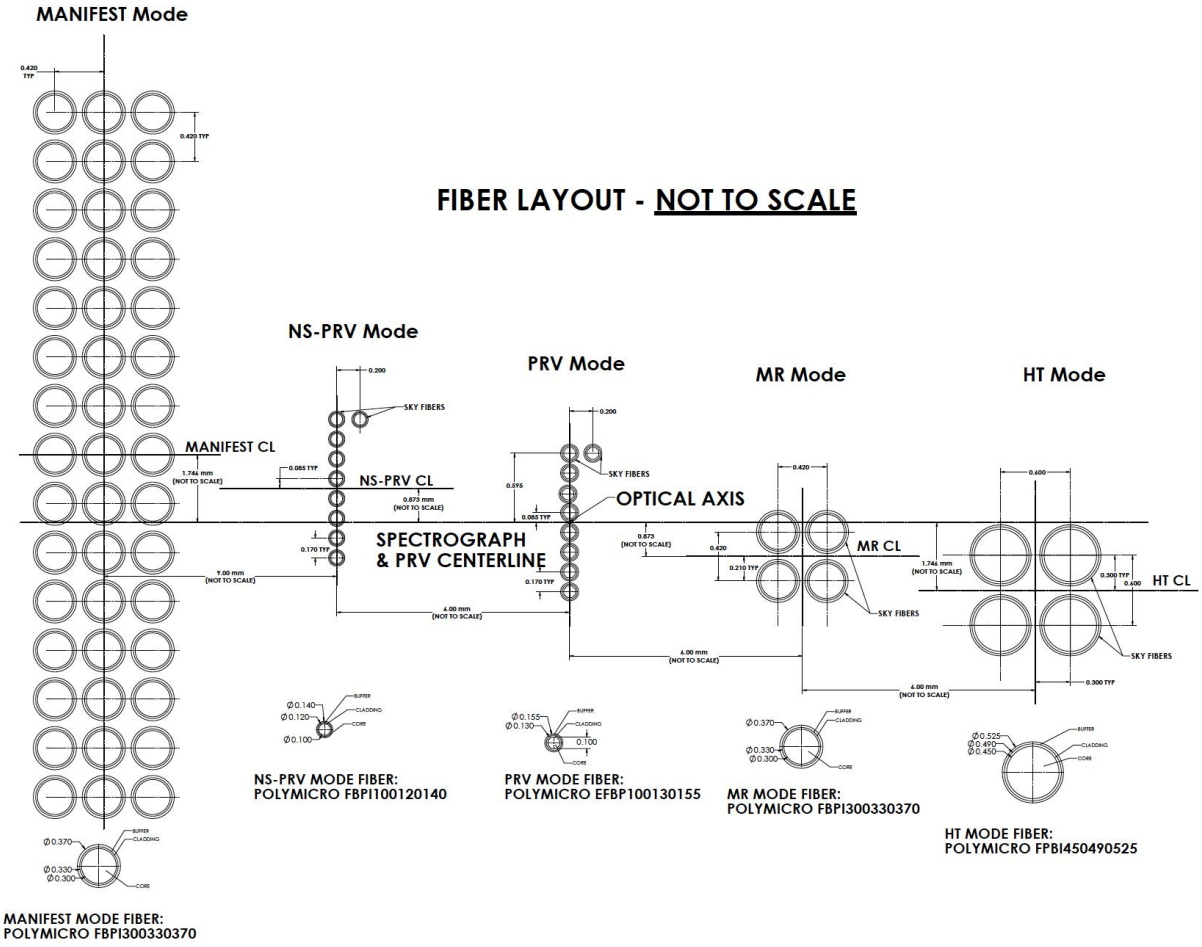

Figure 6: Pseudo-Slit Configuration.

[1] This is one of the reasons why manufacturers advise on illuminating a diffuser with a beam width of at least a few millimeters.

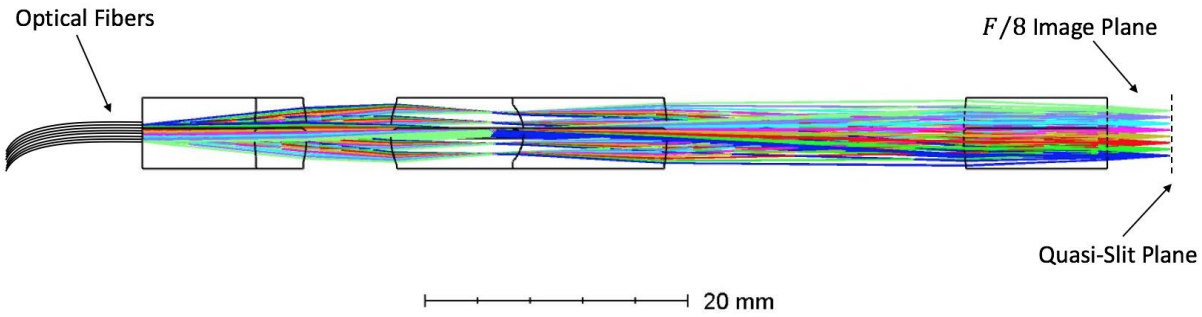

Figure 7: Injection Optics Layout.

Table 2: Flat Field Injection Unit Prescription.

Element	Catalogue Number	Airspace [mm]	
Fiber Collimator		25	Collimator creating a 12mm beam
5° Industrial diffuser	RPC EDC5	90	
Cook Triplet	EO #64-837	86.41	
$0.25\times3.6mm$ slit mask			Coincide with quasi-slit plane

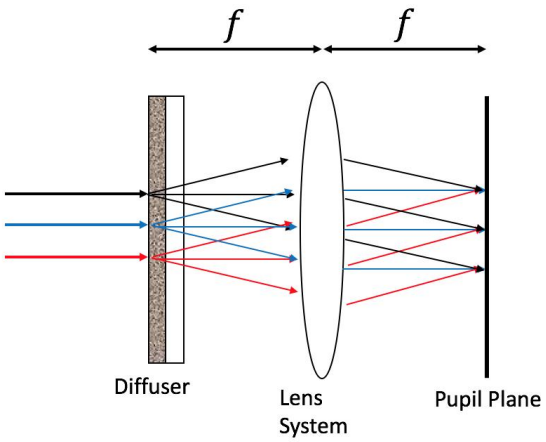

Figure 8:Flat Field Projector.

3. OPTICAL LAYOUT

The G-CLEF spectrograph optical layout, shown in Figure 9, is an asymmetric white pupil echelle design [5,16]. The first element in the optical train, an off-axis-parabolic collimator, sees an F/8 beam emerging from the quasi-slit. The collimated beam has a diameter of 300mm, and illuminates an R4 echelle grating of 306 x 1258mm in size, with 31.6 line/mm ruling density. The location of the grating mid-plane is just behind the slit, 2600mm away from the collimator vertex point. The grating face is tilted at 75.6°, and a true Littrow condition is slightly compromised by a small clockwise rotation of the grating in the plane of Figure 9 ($\gamma = 0.75°$). The dispersed beam hits the collimator in second-

pass and is refocused to a spectral trace in-between the fiber input and the echelle grating. Roughly 40mm before arriving to an intermediate focus point, the beam intercepts a Mangin-type mirror, functioning as a fold mirror and a field flattener, which sends the beam towards a secondary collimator, the pupil transfer mirror (M2). The Mangin mirror is tilted and wedged to eliminate the risk of zero-pass and double-pass ghost images coming into focus on the spectrograph focal plane.

The pupil transfer mirror has a focal length of 1600 mm, or 2/3 of the main collimator (M1). It therefore allows for a smaller dichroic, cross disperser and camera lenses. After beam re-collimation by M2, the beam is split between the red and blue arms of the spectrograph. Each arm includes a VPH grating dispersing the beam in an orthogonal direction to that of the echelle grating's (for the blue arm, the cross disperser is comprised of a prism pre-disperser and a VPH grism, see section 3.1). After cross dispersion, the beams are brought to focus by a 7 and 8-elements cameras with one aspheric surface for the blue and red arm respectively. Large format CCDs record the echellograms imaged by the two cameras (an STA 1600 95.04×95.04mm CCD).

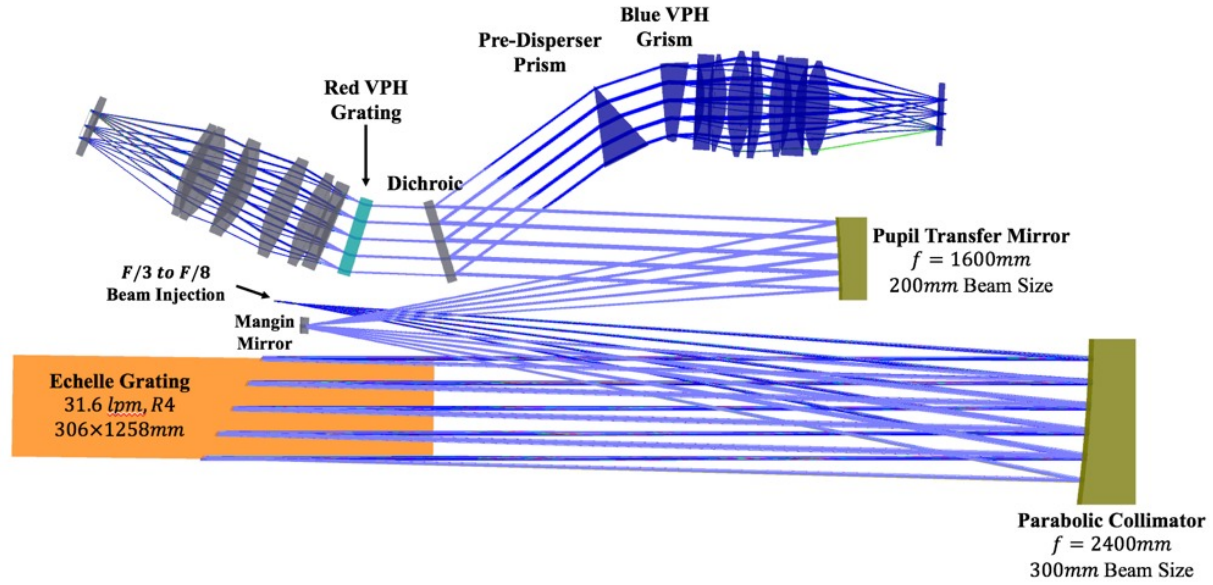

Figure 9: The G-CLEF Spectrograph Optical Layout.

3.1 Quasi Littrow Cross Disperser

The VPH grating dedicated to the blue arm has an estimated peak efficiency of ~85% when fed at Littrow condition. However, simulations performed by the vendor suggest an expected drop of 15% in efficiency at the blue/red ends of the band (*i.e.*, 350nm and 540nm). The efficiency drop is partly attributed to drifting away from the Bragg condition for wavelengths farther away from the peak efficiency. We can increase the efficiency close to the waveband limits by slightly dispersing the beam before it is further dispersed by the VPH grating. The pre-dispersion of the beam is done so that each wavelength is fed slightly closer to its Bragg condition than in the original case in which the incident angle of the VPH has no wavelength dependency. In our approach, the monochromatic beam is collimated, but the polychromatic beam has a wavelength dependent divergence $\alpha(\lambda)$, where α is the Angle of Incidence on the VPH grating. The change in the angle of incidence per wavelength will cause a slight drop in the beam dispersion, which we mitigate by a small increase in the VPH line density wrt a single angle feed. Initial simulations suggest that the pre-dispersed design will yield a 5-10% increase in efficiency at the waveband edges, see Figure 10. This result was backed up by simulations from two of the leading VPH vendors.

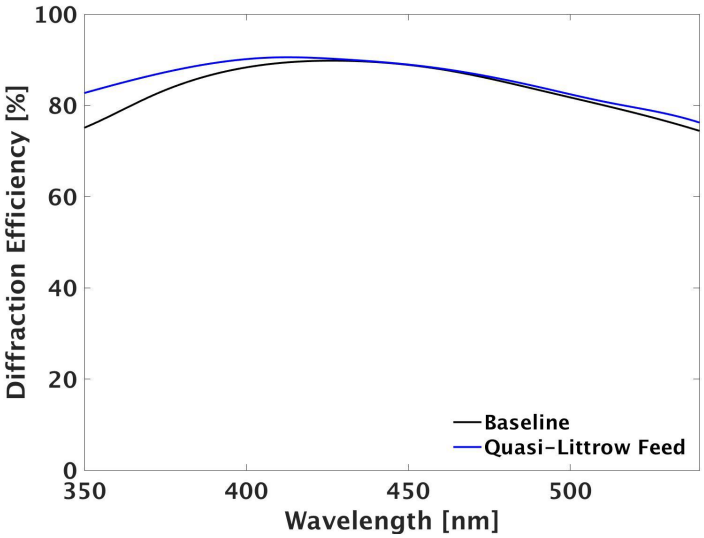

Figure 10: Quasi-Littrow Cross Dispersion offers 5-10% increase in efficiency at the wavebands edges.

3.2 Exposure Meter

In order to obtain radial velocity measurement accuracy of several meters per second and below, it is necessary to correct the measured line of sight velocity to the Solar System barycenter [17]. When aiming at a PRV accuracy of ~10cm/s, the wavelength dependency of this barycentric correction will also play a role [18]. In order to apply this correction, we need to get an exact measurement of the photo-center exposure (*i.e.,* the intensity-weighted time at which the exposure was taken). The G-CLEF Exposure Meter is dedicated to measuring the science exposure wavelength dependent photo-center. The EM feed, shown in Figure 11, is comprised from a flat mirror located at the upper edge of the Echelle grating mask, an off-the-shelf achromat (EO #45-353), and an optical fiber. The mirror reflects ~0.7% of the photons reflected by the system collimator (M1) to the achromat lens which feed an optical fiber channeling the rays outside of the vacuum exposure[2]. The fiber is terminated on the slit module of an off-the-shelf low resolution spectrograph that allows us to monitor the color-dependent photon flux in real time.

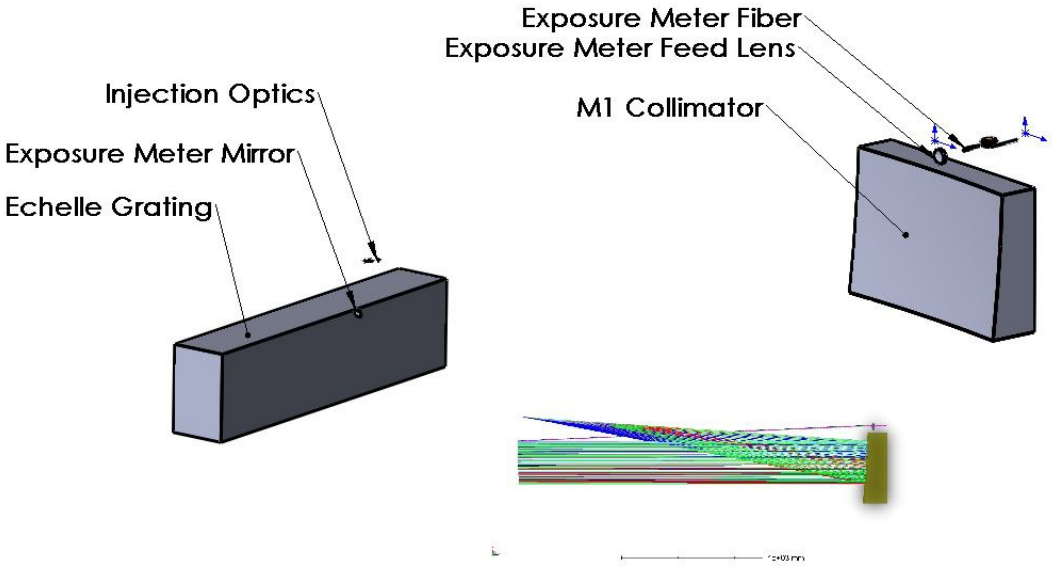

Figure 11: Exposure Meter Feed.

[2] Roughly half of the ray reflected into the Exposure Meter feed are from rays overfilling the grating format.

4. SUMMARY

G-CLEF is a high-resolution optical echelle spectrograph with a PRV capability. Its optical design incorporates novel techniques to allow 10cm/s precision radial velocity measurements without sacrificing other capabilities such as various resolution modes and throughput. The design presented incorporates novel solutions for the instrument fiber feed and spectrograph optical design. G-CLEF is currently in a pre-construction phase, with estimated delivery in 2021 as one of the 1st light instrument for the GMT.

This work has been supported by the GMTO Corporation, a non-profit organization operated on behalf of an international consortium of universities and institutions: Arizona State University, Astronomy Australia Ltd, the Australian National University, the Carnegie Institution for Science, Harvard University, the Korea Astronomy and Space Science Institute, the São Paulo Research Foundation, the Smithsonian Institution, the University of Texas at Austin, Texas A&M University, the University of Arizona, and the University of Chicago.
The authors would also like to thank to Gabor Furesz, Harland Epps, and Stuart I. Barnes for their kind advice and contribution to the project.

REFERENCES

[1] Szentgyorgyi, A., et al., "The GMT-Consortium Large Earth Finder (G-CLEF): An Optical Echelle Spectrograph for the Giant Magellan Telescope (GMT)", *Proc. SPIE* 9908, Ground-based and Airborne Instrumentation for Astronomy VI (2016).
[2] Fanson, J., et al., "Overview and status of the Giant Magellan telescope project", Proc. SPIE 10700-34 (2018).
[3] Lawrence, J. S., et al., "The MANIFEST prototyping design study", *Proc. SPIE* 9908, Ground-based and Airborne Instrumentation for Astronomy VI (2016).
[4] Mueller, M. A., et al., "The opto-mechanical design of the GMT-consortium large earth finder (G-CLEF)", *Proc. SPIE* 9147, Ground-based and Airborne Instrumentation for Astronomy VI (2016).
[5] Ben-Ami S., et al., "The optical design of the G-CLEF Spectrograph: the first light instrument for the GMT", *Proc. SPIE* 9908, Ground-based and Airborne Instrumentation for Astronomy VI (2016).
[6] Fisher, D. A., et al., "State of the Field: Extreme Precision Radial Velocities", Publications of the Astronomical Society of the Pacific, Volume 128, Issue 964 (2016).
[7] Szentgyorgyi, A., et al., "The GMT-consortium large earth finder (G-CLEF): an optical echelle spectrograph for the Giant Magellan telescope (GMT)", *Proc. SPIE* 10702, Ground-based and Airborne Instrumentation for Astronomy VII (2018).
[8] Mueller, M. A., et al., "The opto-mechanical design of the GMT-consortium large Earth finder (G-CLEF)", *Proc. SPIE* 10702, Ground-based and Airborne Instrumentation for Astronomy VII (2018).
[9] Mueller, M. A., et al., "Precision thermal control of the GMT-consortium large earth finder (G-CLEF)", *Proc. SPIE* 10702, Ground-based and Airborne Instrumentation for Astronomy VII (2018).
[10] Evans, I. N., et al., "The preliminary design of the G-CLEF spectrograph instrument device control system", *Proc. SPIE* 10707, Ground-based and Airborne Instrumentation for Astronomy VII (2018).
[11] Oh, J., S., et al., "Detailed design of the G-CLEF flexure control camera subsystem"", *Proc. SPIE* 10707, Ground-based and Airborne Instrumentation for Astronomy VII (2018).
[12] Clayton, C. A., "The implications of image scrambling and focal ratio degradation in fibre optics on the design of astronomical instrumentation", A&A 213, 502–515 (1989).
[13] Chazelas, B. et al., "Optical Fibers for Precise Radial Velocities: An Update", *Proc. SPIE* 8450, Ground-based and Airborne Instrumentation for Astronomy IV (2012).
[14] Schroeder, D. J., "Astronomical Optics", *Academic Press* (2000).
[15] Jurgenson, C., et al., "EXPRES: A Next Generation RV Spectrograph in the Search for Earth-like Worlds", *Proc. SPIE* 9908, Ground-based and Airborne Instrumentation for Astronomy VI (2016).
[16] Furesz, G. et al., "The G-CLEF spectrograph optical design", *Proc. SPIE* 9147, Ground-based and Airborne Instrumentation for Astronomy V (2014).

[17] Wright, J. T., and Eastman, J. D., "Barycentric Corrections at 1cm/s for Precise Doppler Velocities", Publications of the Astronomical Society of the Pacific, Volume 126, Issue 943 (2014).
[18] Blackman, R.T., Szymkowiak, A.E., Fischer, D.A., and Jurgensen, C.A., "Accounting for Chromatic Atmospheric Effects on Barycentric Corrections", The Astrophysical Journal, Volume 837, Issue 1 (2017).